Cell Metabolism, Volume *23*

Supplemental Information

Mitochondrial OXA Translocase Plays a Major Role in Biogenesis of Inner-Membrane Proteins

Sebastian B. Stiller, Jan Höpker, Silke Oeljeklaus, Conny Schütze, Sandra G. Schrempp, Jens Vent-Schmidt, Susanne E. Horvath, Ann E. Frazier, Natalia Gebert, Martin van der Laan, Maria Bohnert, Bettina Warscheid, Nikolaus Pfanner, and Nils Wiedemann

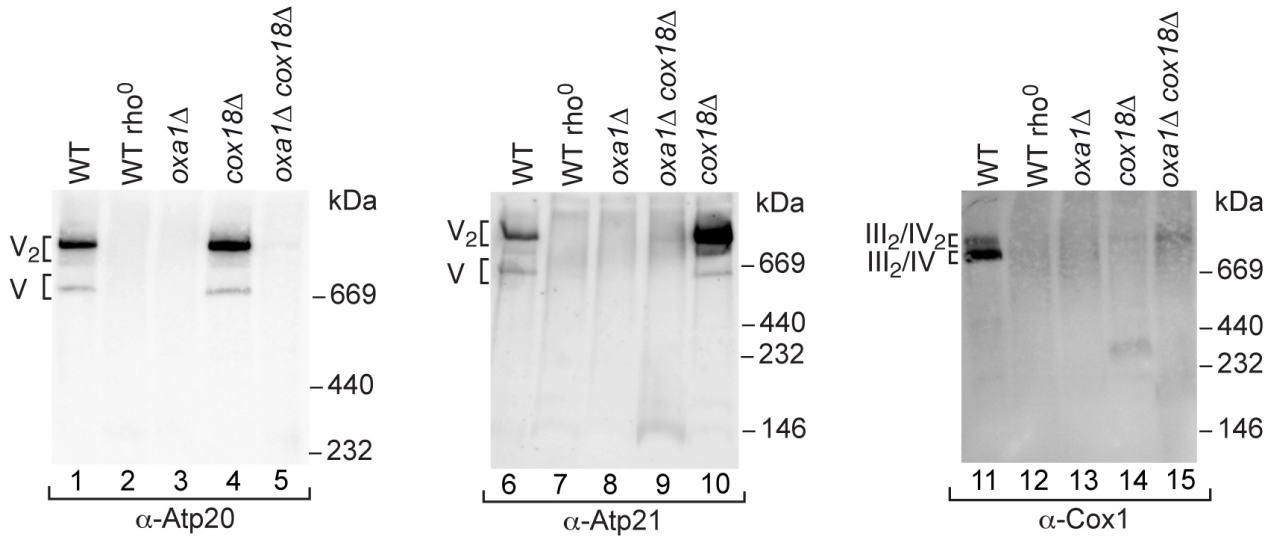

Figure S1. Defects of Oxidative Phosphorylation Complexes in Oxa1-deficient Mitochondria, Related to Figure 1

Mitochondria were isolated from wild-type (WT), WT rho^0, *oxa1*Δ, *cox18*Δ and *oxa1*Δ *cox18*Δ yeast, lysed with digitonin and analyzed by blue native electrophoresis and immunoblotting with the indicated antisera. V, complex V (F_1F_o-ATP synthase); V_2, ATP synthase dimer; III_2/IV and III_2/IV_2, respiratory chain supercomplexes of complex III and complex IV.

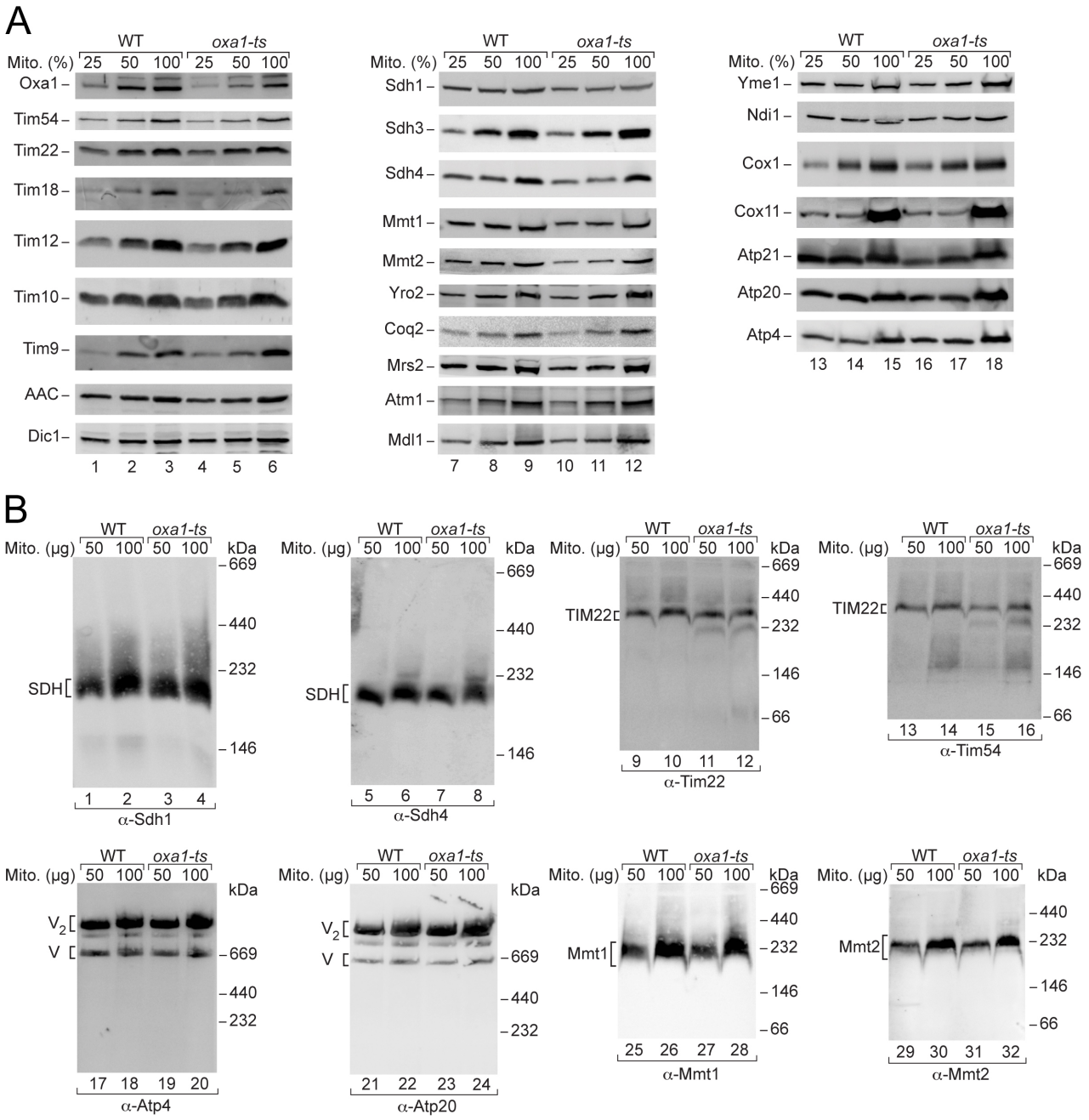

Figure S2. Characterization of Mitochondria Isolated After Growth of *oxa1-ts* Yeast at Permissive Conditions, Related to Figure 2

(A) Wild-type (WT) and *oxa1-ts* yeast cells were grown at 21°C. Mitochondria were isolated and protein levels were analyzed by SDS-PAGE and immunoblotting with antisera against the indicated proteins. Mito., total mitochondrial protein; 100% represents 160 µg protein (80 µg for Tim54, Tim22, Tim12, Tim10, AAC, Dic1, Coq2, Atm1, Mdl1 and Ndi1; 40 µg for Oxa1, Tim9 and Sdh3).

(B) Mitochondria isolated from WT and *oxa1-ts* cells were lysed with 1% digitonin and subjected to blue native electrophoresis and immunoblotting. Without a heat shock, *oxa1–ts* mitochondria have a mild assembly defect, evidenced by a sub-assembled TIM22 complex of ~230 kDa of low abundance (lanes 11, 12, 15 and 16) and reduced levels of the [^{35}S]Tim18-Sdh3 assembly intermediate seen in Figure 2C.

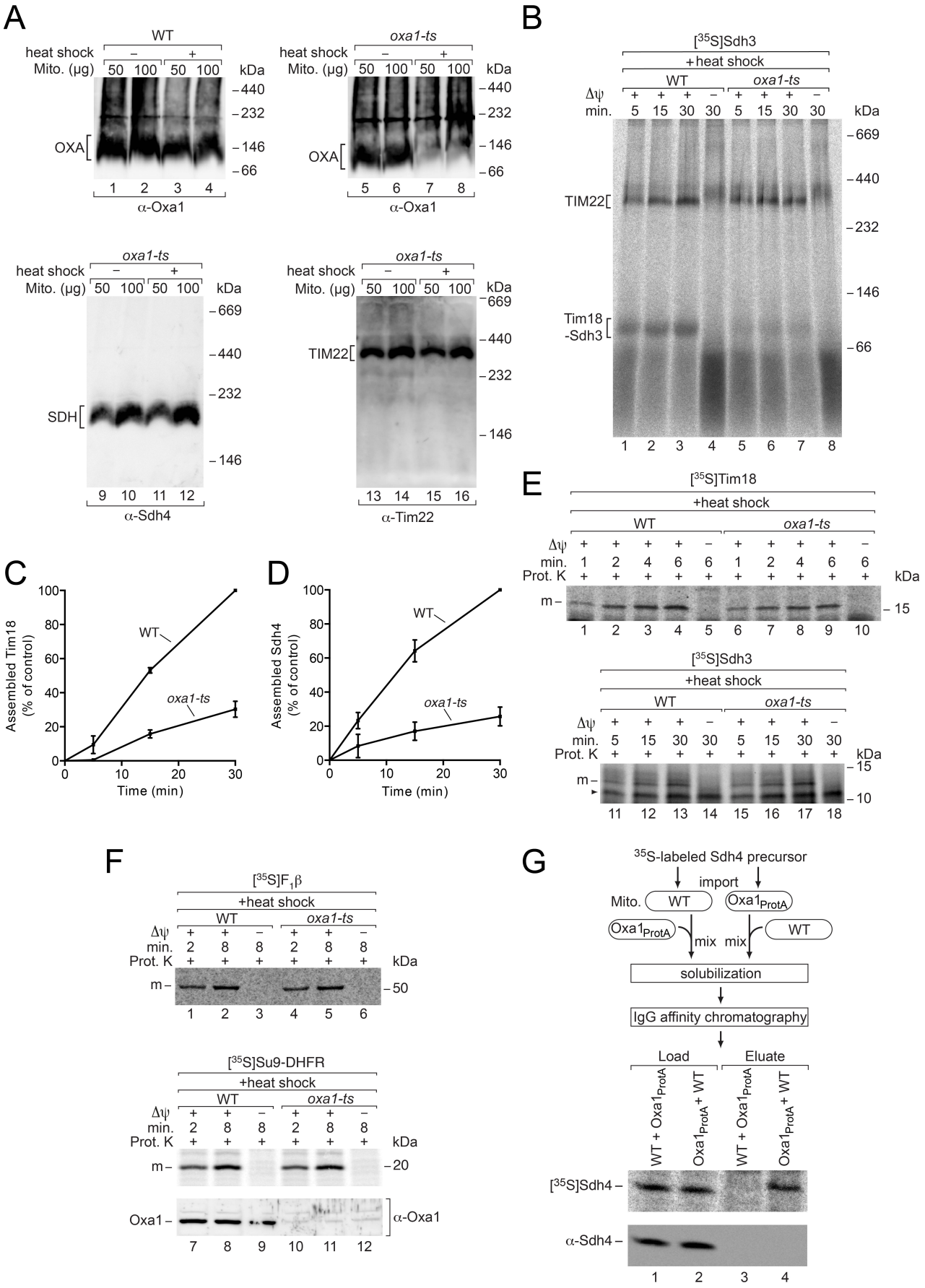
A
WT
oxa1-ts
heat shock
Mito. (µg)
50 100 50 100
kDa
440
232
146
66
OXA
1 2 3 4
α-Oxa1
5 6 7 8
α-Oxa1
669
SDH
9 10 11 12
α-Sdh4
TIM22
13 14 15 16
α-Tim22
B
[35S]Sdh3
+heat shock
Δψ
min.
5 15 30 30 5 15 30 30
TIM22
Tim18
-Sdh3
1 2 3 4 5 6 7 8
C
Assembled Tim18
(% of control)
WT
oxa1-ts
Time (min)
D
Assembled Sdh4
(% of control)
E
[35S]Tim18
Prot. K
m
1 2 3 4 5 6 7 8 9 10
[35S]Sdh3
11 12 13 14 15 16 17 18
F
[35S]F1β
[35S]Su9-DHFR
Oxa1
7 8 9 10 11 12
G
35S-labeled Sdh4 precursor
import
Mito.
Oxa1ProtA
mix
solubilization
IgG affinity chromatography
Load
Eluate
WT + Oxa1ProtA
Oxa1ProtA + WT
[35S]Sdh4
α-Sdh4
1 2 3 4

Figure S3

Figure S3. Characterization of Import and Assembly in *oxa1-ts* Mitochondria, Related to Figure 2

(A) Wild-type (WT) or *oxa1-ts* mitochondria were suspended in import buffer supplemented with 4 mM ATP, followed by either a 12 min heat shock at 37°C or incubation at 25°C. Mitochondria were washed, lysed with digitonin and analyzed by blue native electrophoresis and immunoblotting.

(B) Assembly of Sdh3 in WT and *oxa1-ts* mitochondria. Isolated mitochondria were heat-shocked for 12 min at 37°C. [^{35}S]Sdh3 precursor was imported in the presence of non-radiolabeled Tim18 (Gebert et al., 2011) at 25°C, followed by proteinase K treatment. Formation of the Tim18-Sdh3 assembly intermediate and the TIM22 complex were analyzed by blue native electrophoresis and digital autoradiography. Assembly of [^{35}S]Sdh3 into the TIM22 complex requires the presence of sufficient amounts of Tim18 precursor (supplied in chemical amounts from wheat germ lysate; Gebert et al., 2011). The activity of Oxa1 is rate-limiting for the first assembly step (Tim18-Sdh3 intermediate); [^{35}S]Sdh3 reaching this intermediate is then rapidly assembled into the TIM22 complex.

(C, D) ^{35}S-labeled Tim18 (C) or Sdh4 precursor (D) were imported into in vitro heat-treated (12 min at 37°C) WT and *oxa1-ts* mitochondria at 25°C (C) or 30°C (D). Non-imported precursor was removed by addition of proteinase K. ^{35}S-labeled assembled complexes were analyzed by blue native electrophoresis and quantified by digital autoradiography (mature TIM22 complex (C) or sum of Sdh3-Sdh4 intermediate and mature SDH complex (D)). The assembly yield in WT mitochondria after 30 min import was set to 100% (control). The results are shown as mean ± SEM (n=3 independent experiments; mean with range of two independent experiments for the 15 min time point of (C)).

(E) Radiolabeled Tim18 (lanes 1-10) or Sdh3 precursors (lanes 11-18) were imported into WT and *oxa1-ts* mitochondria at 25°C (Tim18) or 30°C (Sdh3) for the indicated periods. Mitochondria were heat-shocked for 12 min at 37°C before the import reaction. Non-imported precursors were removed by proteinase K. Import was analyzed by SDS-PAGE and autoradiography. m, mature form; arrowhead, unspecific band.

(F) WT and *oxa1-ts* mitochondria were subjected to an in vitro heat shock (37°C) and incubated with the ^{35}S-labeled precursors of $F_1\beta$ (F_1-ATPase subunit β /Atp2) and Su9-DHFR (fusion protein between the presequence of *Neurospora crassa* F_o-ATPase subunit 9 and mouse dihydrofolate reductase) at 25°C, followed by treatment with proteinase K. The mitochondria were analyzed by SDS-PAGE and autoradiography (upper and middle panels) or immunodecoration (lower panel).

(G) [^{35}S]Sdh4 precursor was imported into WT or $Oxa1_{ProtA}$ mitochondria for 8 min at 30°C. After removal of non-imported precursor by proteinase K, [^{35}S]Sdh4-containing mitochondria were mixed with unlabeled mitochondria of the other type as indicated. Mitochondria were solubilized with 1% digitonin and subjected to IgG affinity chromatography, followed by elution with TEV protease. Samples were analyzed by SDS-PAGE and autoradiography (upper panel) or immunodecoration (lower panel). Load 0.15%; eluate 100%. [^{35}S]Sdh4 was only co-purified with tagged Oxa1 when it was imported into $Oxa1_{ProtA}$ mitochondria, excluding a post-lysis interaction of the precursor with $Oxa1_{ProtA}$.

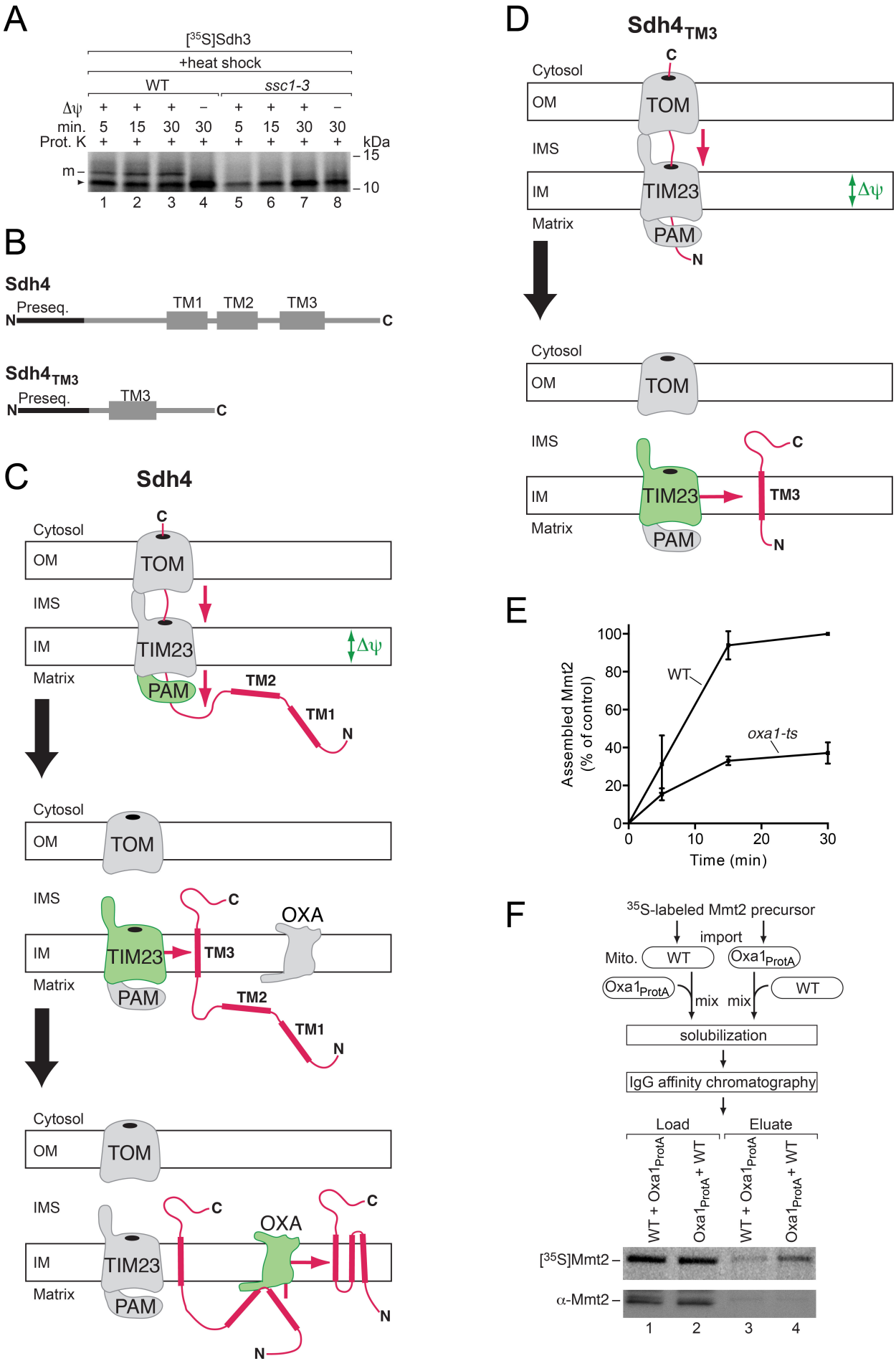
A
[35S]Sdh3
+heat shock
WT
ssc1-3
Δψ + + + − + + + −
min. 5 15 30 30 5 15 30 30
Prot. K + + + + + + + +
kDa
15
10
m
1 2 3 4 5 6 7 8
B
Sdh4
Preseq.
TM1 TM2 TM3
N C
Sdh4TM3
Preseq.
TM3
N C
C
Sdh4
Cytosol
OM
IMS
IM
Matrix
TOM
TIM23
PAM
Δψ
TM2
TM1
N
C
OXA
TM3
D
Sdh4TM3
Cytosol
OM
IMS
IM
Matrix
TOM
TIM23
PAM
Δψ
N
C
TM3
E
Assembled Mmt2 (% of control)
100
80
60
40
20
0
WT
oxa1-ts
0 10 20 30
Time (min)
F
35S-labeled Mmt2 precursor
import
Mito.
WT
Oxa1ProtA
mix
solubilization
IgG affinity chromatography
Load
Eluate
WT + Oxa1ProtA
Oxa1ProtA + WT
[35S]Mmt2
α-Mmt2
1 2 3 4

Figure S4

Figure S4. Import Experiments into Mutant Mitochondria and Hypothetical Model of the Sdh4 Sorting Pathway, Related to Figures 3 and 4

(A) Isolated wild-type (WT) and *ssc1-3* mitochondria were heat-shocked for 12 min at 37°C, followed by import of radiolabeled Sdh3 precursor at 30°C. After removal of non-imported precursor by proteinase K, samples were analyzed by SDS-PAGE and autoradiography. m, mature form; arrowhead, unspecific band.

(B) Scheme of presequence (Preseq.) and transmembrane (TM) segments of Sdh4 and $Sdh4_{TM3}$.

(C, D) Hypothetical model of the mitochondrial sorting pathways of Sdh4 (C) and $Sdh4_{TM3}$ (D). OM, outer mitochondrial membrane; IMS, intermembrane space; IM, inner mitochondrial membrane.

(E) [^{35}S]Mmt2 was imported into in vitro heat-shocked (12 min at 37°C) WT and *oxa1-ts* mitochondria, followed by proteinase K treatment. Mitochondria were analyzed by blue native electrophoresis and Mmt2 assembly was quantified by digital autoradiography. The assembly yield in WT mitochondria after 30 min import was set to 100% (control). The results are shown as mean ± SEM (n=3 independent experiments).

(F) [^{35}S]Mmt2 precursor was imported into WT or $Oxa1_{ProtA}$ mitochondria for 10 min at 30°C and analyzed as described in the legend of Figure S3G, revealing that [^{35}S]Mmt2 was specifically co-purified with tagged Oxa1 only when it was imported into $Oxa1_{ProtA}$ mitochondria.

SUPPLEMENTAL EXPERIMENTAL PROCEDURES

Generation of Yeast Strains and Cloning

Table S2 summarizes the *S. cerevisiae* strains used. Individual chromosomal deletions of *COX18* and *OXA1* were generated by their substitution with a *His3MX6* cassette (Longtine et al., 1998). For chromosomal deletion of the *COX18* gene in *oxa1*Δ yeast, an *URA3* cassette was introduced (Berben et al., 1991). For PCR amplification of integration cassettes, flanked by sequences homologous to the 5' untranslated region (UTR) and 3'-UTR of the selected open reading frame, the KOD Hot Start Master Mix (Merck Millipore) was used. For transformation of yeast strains the lithium acetate/single-stranded carrier DNA/polyethylene glycol method (Gietz and Woods, 2002) was employed and verified by PCR or Western blot analysis. The $Sdh4_{TM3}$ precursor consists of the N-terminal Sdh4 presequence (amino acid residues 1-31 according to Vögtle et al., 2009) followed by the C-terminus of Sdh4 (amino acid residues 121-181). To generate the [^{35}S]Mmt2 precursor, a PCR product encoding amino acid residues 1 to 450 (including presequence and all five TMs) was used.

Plasmids Used in This Study

Name	Backbone	Insert	Source	Number
pGEM-AAC	pGEM-4Z	*S. cerevisiae* AAC2	Wiedemann et al., 2001	1039
pGEM-Dic1	pGEM	BamHI-DIC1 (*S. cerevisiae*)-EcoRI	Pfanner/ Wiedemann Labs	A32
pGEM-Su9-DHFR	pGEM	EcoRI-Su9(1-69, *N. crassa*)-DHFR(mouse)-HindIII	Pfanner/ Wiedemann Labs	SO2
pGEM-$F_1\beta$	pSP64	HindIII-$F_1\beta$ (*S. cerevisiae*)-HindIII	Pfanner/ Wiedemann Labs	F01
YDp-U	pUC9HStop	HindIII-URA3-SmaI	Berben et al., 1991	X45
pFA6a-His3MX6	pFA6	BamHI-P_{TEV}-his5+ (*S. pombe*)-T_{TEV}-EcoRI	Wach, 1996	1424

PCR Primers Used in This Study

Name	Sequence (5'→ 3')	Description
COQ2 SP6 fw	GATCGATTTAGGTGACACTATAGAAGCGGC CACCATGTTTATTTGGCAGAGAAAGAGTATT TTAC	Generation of SP6-Coq2 PCR template for RNA synthesis
COQ2 rev	CTACAAGAATCCAAACAGTCTCAAG	
SP6_Sdh4_f_ SBS	TCGATTTAGGTGACACTATAGAATACGCCGC CGCCGATCTTTCCTACGCTTTCG	Generation of SP6-Sdh4 PCR template for RNA synthesis; generation of SP6-$Sdh4_{TM3}$ construct
Sdh4_rc_SBS	CTACTTCTTGGCTTCAATC	
Sp6Tim18	TCGATTTAGGTGACACTATAGAATACGCCGC CGCCATGCTATTGT	Generation of SP6-Tim18 PCR template for RNA synthesis
Tim18rc	TATGGGTGAGTCAGTTTCTTC	
MMT2 SP6 fw	GATCGATTTAGGTGACACTATAGAAGCGGC CACCATGCTACGGATAAGTATTGACTCTATC	Generation of SP6-Mmt2 PCR template for RNA synthesis
MMT2 rev (Δ451)	TTACATCAACAAACTCGACGTCCAC	
Sdh3_SP6_fwd	TCGATTTAGGTGACACTATAGAATACGCCGC CGCCGCATAGAAATCTCAGGACC	Generation of SP6-Sdh3 PCR template for RNA synthesis
Sdh3_rev	TCATAAAGTTAATAAATAAGTACCGAG	
Sdh4_linker_f	ATTTCTGAAAGAGTTTATGGTG	Generation of SP6-$Sdh4_{TM3}$ construct
Sdh4_linker_rev	CACCATAAACTCTTTCAGAAATGCTCTTCTTA GCGGTAGAC	
Mmt1_RWG_ sense	CTTTAAGAAGGAGATATACCATGTTAAGAAT CTGCGTAAAAAGG	Generation of Mmt1 template DNA using the RTS™ Wheat Germ LinTempGenSet
Mmt1_RWG_anti	TGATGATGAGAACCCCCCCCTCAAATATGAG TATTCGTATGG	
Tim18_RWG_ sense	CTTTAAGAAGGAGATATACCATGCTATTGTTT CCTGGCTTG	Generation of Tim18 template DNA using the RTS™ Wheat Germ LinTempGenSet
Tim18_RWG_ anti	TGATGATGAGAACCCCCCCCTCAGTTTCTTC CAAATATATACAA	
Cox18d_YDp_f2	AAGGTCCAAGGATAGGAAAATTTCAAGATAA AGTATGGCATTGAATTCCCGGGGATCC	Genomic deletion of *COX18* ORF
Cox18d_YDp_r2	CTGATGTAGAATTACATATCCTATCTATGCGT CAGCTTCACGCTAGCTTGGCTGCAG	
Cox18_test_f	CTACCGTCCAGTAATTC	Verification of genomic *COX18* deletion
Cox18_test_r	GTTTATTTACAAGCTGATGTAG	

Mass Spectrometry and Data Analysis

For the SILAC-based quantitative MS analysis of wild-type yeast and an *oxa1 cox18* double deletion strain (*oxa1*Δ *cox18*Δ), equal amounts of Lys8/Arg10-labeled wild-type and non-isotopically labeled mutant cells were mixed based on optical densities before isolation of crude mitochondria. Proteins of the mitochondrial fraction (4 µg protein per LC/MS run) were precipitated with acetone, resuspended in 8 M urea/50 mM NH_4HCO_3, and subjected to reduction with TCEP and alkylation with iodoacetamide followed by

tryptic digestion as described (Lytovchenko et al., 2014). The generated peptides were analyzed by LC/MS using an Ultimate 3000 RSLCnano HPLC system (Thermo Scientific, Dreieich, Germany) directly coupled to an Orbitrap Elite mass spectrometer (Thermo Scientific, Bremen, Germany). Peptides were preconcentrated and washed on a 5 mm x 0.3 mm PepMap™ C18 µ-precolumn (Thermo Scientific) for 25 – 30 min and separated on a 50 cm x 75 µm C18 reversed-phase nano LC column (Acclaim PepMap™ RSLC column; particle size 2 µm; pore size 100 Å; Thermo Scientific) at 40°C using a binary solvent system consisting of 0.1% (v/v) formic acid (solvent A) and 50% (v/v) methanol/30% (v/v) acetonitrile in 0.1% (v/v) formic acid (solvent B). For peptide elution, a linear gradient of 5 – 62% solvent B followed by 62 – 90% solvent B was applied; the flow rate was 250 nl/min. The Orbitrap Elite instrument was operated essentially as described (Hünten et al., 2015).

For protein identification and quantification, mass spectrometric data were processed using MaxQuant (version 1.3.0.5; Cox and Mann, 2008) and Andromeda (Cox et al., 2011) as described (Lytovchenko et al., 2014). The *Saccharomyces* Genome Database (SGD; www.yeastgenome.org) was used for the database search. The option "Re-quantify" implemented in MaxQuant and applied to our data analysis generally allows for the calculation of a SILAC ratio in case a peptide is only present in the isotope-labeled or unlabeled form by assigning a peptide intensity for the missing counterpart from the background signals in MS spectra at the expected *m/z* value. A list of all proteins detected is provided in Table S1.

The presence or absence of a presequence was predicted using TargetP 1.1 (for Atm1 and Nde2) (Emanuelsson et al., 2000; Nielsen et al., 1997) or evaluated according to Vögtle et al. (2009) (for Mdl2, Mmt2, Coq2, Sdh3, Sdh4, Cox15 and Pam17), Vukotic et al. (2012) (for Rcf2) and Bohnert et al. (2015) (for Mic10). Transmembrane segments were predicted by using TMpred (Hofmann and Stoffel, 1993).

Analysis of Proteins Using SDS-PAGE and Blue Native Electrophoresis

For separation of proteins using Tricine-SDS-PAGE, 10-16.5% discontinuous polyacrylamide gels (1 M Tris-HCl [pH 8.45], 0.1% [w/v] SDS) were employed using cathode buffer (100 mM Tris, 100 mM Tricine, 0.1% [w/v] SDS [pH 8.25]) and anode buffer (200 mM Tris-HCl [pH 8.9]). Alternatively, the non-polymerized separating gel (16%/6 M urea) was overlaid with 10% gel (w/o glycerol) that, after polymerization, was covered with a 4% sample gel (AB-6) (Schägger, 2006). For protein separation using the Tris-glycine buffer system, 12% or 16% discontinuous polyacrylamide gels were employed (Laemmli, 1970).

Steady state protein levels of mitochondria were analyzed by lysis of 10–320 µg of mitochondria (protein amount) with Laemmli buffer (2% [w/v] SDS, 10% [v/v] glycerol, 60

mM Tris-HCl [pH 6.8], 0.01% [w/v] bromphenol blue, 1% [v/v] β-mercaptoethanol, 1 mM PMSF) followed by electrophoretic separation and Western blotting onto polyvinylidene fluoride membranes. Protein levels were determined using immunodecoration with enhanced chemiluminescence (Haan and Behrmann, 2007).

For blue native electrophoresis, 6–16.5% or 3–13% discontinuous polyacrylamide gels (50 mM Bis Tris-HCl [pH 7.0], 67 mM ε-amino n-caproic acid) were used for separation (cathode buffer: 50 mM Tricine [pH 7.0], 15 mM Bis-Tris, (0.02% [w/v] Coomassie G); anode buffer: 50 mM Bis-Tris-HCl [pH 7.0]). For the analysis of steady state levels of protein complexes, 50–100 µg of mitochondria (protein amount) were solubilized in 1% digitonin buffer (1% [w/v] digitonin, 20 mM Tris-HCl [pH 7.4], 0.1 mM EDTA, 50 mM NaCl, 10% [v/v] glycerol, 1 mM PMSF) and incubated for 15 min on ice. After removal of non-solubilized material by centrifugation, blue native loading dye was added (final concentration: 0.5% [w/v] Coomassie G-250, 50 mM ε-amino n-caproic acid, 100 mM Bis-Tris-HCl [pH 7.0]) and the samples were loaded onto the blue native gel. After the running front had migrated into the running gel, the cathode buffer was exchanged with the buffer without Coomassie G (Schägger and von Jagow, 1991; Schägger et al., 1994).

IgG Affinity Chromatography

Radiolabeled Sdh4 or Mmt2 precursor was imported into 1.2 mg (protein amount) of wild-type (WT, YPH499) or $Oxa1_{ProtA}$ mitochondria for 8–10 min at 30°C. Non-imported precursor was digested with proteinase K. Mitochondria were pelleted and the supernatant was discarded. To remove residual traces of radioactive precursor proteins, mitochondria were resuspended in SEM buffer and subjected to another clarifying spin. Subsequently WT or $Oxa1_{ProtA}$ mitochondria were mixed with 1.2 mg of untreated mitochondria of the other type. The mitochondrial mixture was solubilized in 2 ml of solubilization buffer (20 mM Tris-HCl [pH 7.4], 50 mM NaCl, 0.1 mM EDTA, 10% [v/v] glycerol, 1% [w/v] digitonin, 1.5 mM PMSF, 1x EDTA-free Protease Inhibitor Cocktail [Roche]). Non-solubilized material was pelleted by centrifugation and a portion of the soluble fraction was taken as load. 100 µl of 50% slurry human IgG-coupled Sepharose beads were equilibrated with solubilization buffer and added to solubilized mitochondria followed by 90 min head-over-head incubation at 4°C. Beads were transferred to a mobicol column and washed 15-times with 500 µl of wash buffer (20 mM Tris-HCl [pH 7.4], 60 mM NaCl, 0.5 mM EDTA, 10% [v/v] glycerol, 0.3% [w/v] digitonin, 1.5 mM PMSF, 1x EDTA-free Protease Inhibitor Cocktail [Roche]). Proteins specifically bound to IgG beads via $Oxa1_{ProtA}$ were eluted by incubation with tobacco etch virus (TEV) protease under vigorous shaking at 4°C overnight. Samples were subjected to SDS-PAGE and Western Blotting followed by autoradiography and antibody decoration.

Antibodies Used in This Study

Antigen	Dilution	Number	Secondary antibody
Aac2	1:500 TBS-T + 5% milk	GR3617-7	anti-rabbit
Atm1	1:200 TBS-T + 5% milk	GR1641-7	anti-rabbit
Atp4	1:500 TBS-T + 5% milk	GR1970-4	anti-rabbit
Atp20	1:500 TBS-T + 5% milk	GR1516-4	anti-rabbit
Dic1	1:200 TBS-T + 5% milk	GR2054-5	anti-rabbit
Coq2	1:50 TBS	GR2097; affinity purified e1-e9	anti-rabbit
Cox1	1:400 TBS-T + 5% milk	GR1538-4	anti-rabbit
Cox11	1:200 TBS-T + 5% milk	GR1102-2	anti-rabbit
Mdl1	1:200 TBS-T + 5% milk	GR1518-7	anti-rabbit
Mdj2	1:400 TBS-T + 5% milk	GR1842-7	anti-rabbit
Mia40	1:750 TBS-T + 5% milk	B315	anti-rabbit
Mir1	1:1000 TBS-T + 5% milk	171-5	anti-rabbit
Mmt1	1:50 TBS	GR2049; affinity purified e1-e6	anti-rabbit
Mmt2	1:25 TBS	GR2090; affinity purified ++	anti-rabbit
Mrs2	1:25 TBS	GR2093; affinity purified e5-e8	anti-rabbit
Ndi1	1:200 TBS-T + 5% milk	GR809-4	anti-rabbit
Oxa1	1:100 TBS-T + 5% milk	262-6	anti-rabbit
Sam50	1:300 TBS-T + 5% milk	B312-14	anti-rabbit
Sdh1	1:1000 TBS-T + 5% milk	GR1849-3	anti-rabbit
Sdh3	1:250 TBS-T + 5% milk	GR2434-5	anti-rabbit
Sdh4	1:2000 TBS-T + 5% milk	GR1855-3	anti-rabbit
Pam16	1:200 TBS-T + 5% milk	GR750-6	anti-rabbit
Tim9	1:250 TBS-T + 5% milk	GR2013-5	anti-rabbit
Tim10	1:500 TBS-T + 5% milk	217-8	anti-rabbit
Tim11/ Atp21	1:400 TBS-T + 5% milk	138-9	anti-rabbit
Tim12	1:250 TBS-T + 5% milk	GR906-7	anti-rabbit
Tim13	1:1000 TBS-T + 5% milk	238-5	anti-rabbit
Tim18	1:1000 TBS-T + 5% milk	233-7	anti-rabbit
Tim22	1:500 TBS-T + 5% milk	164-4	anti-rabbit
Tim23	1:500 TBS-T + 5% milk	133-9	anti-rabbit
Tim50	1:500 TBS-T + 5% milk	257-8	anti-rabbit
Tim54	1:1000 TBS-T + 5% milk	215-6	anti-rabbit
Tom40	1:750 TBS-T + 5% milk	168-4	anti-rabbit
Yme1	1:400 TBS-T + 5% milk	GR1435-3	anti-rabbit
Yro2	1:200 TBS-T + 5% milk	GR2095-4	anti-rabbit

SUPPLEMENTAL REFERENCES

Berben, G., Dumont, J., Gilliquet, V., Bolle, P.A., and Hilger, F. (1991). The YDp plasmids: a uniform set of vectors bearing versatile gene disruption cassettes for *Saccharomyces cerevisiae*. Yeast *7*, 475–477.

Bohnert, M., Zerbes, R.M., Davies, K.M., Mühleip, A.W., Rampelt, H., Horvath, S.E., Boenke, T., Kram, A., Perschil, I., Veenhuis, M., et al. (2015). Central role of Mic10 in the mitochondrial contact site and cristae organizing system. Cell Metab. *21*, 747–755.

Cox, J., and Mann, M. (2008). MaxQuant enables high peptide identification rates, individualized p.p.b.-range mass accuracies and proteome-wide protein quantification. Nature Biotechnol. *26*, 1367–1372.

Cox, J., Neuhauser, N., Michalski, A., Scheltema, R.A., Olsen, J.V., and Mann, M. (2011). Andromeda: a peptide search engine integrated into the MaxQuant environment. J. Proteome Res. *10*, 1794–1805.

Emanuelsson, O., Nielsen, H., Brunak, S., and von Heijne, G. (2000). Predicting subcellular localization of proteins based on their N-terminal amino acid sequence. J. Mol. Biol. *300*, 1005–1016.

Frazier, A.E., Dudek, J., Guiard, B., Voos, W., Li, Y., Lind, M., Meisinger, C., Geissler, A., Sickmann, A., Meyer, H.E., et al. (2004). Pam16 has an essential role in the mitochondrial protein import motor. Nat. Struct. Mol. Biol. *11*, 226–233.

Frazier, A.E., Taylor, R.D., Mick, D.U., Warscheid, B., Stoepel, N., Meyer, H.E., Ryan, M.T., Guiard, B., and Rehling, P. (2006). Mdm38 interacts with ribosomes and is a component of the mitochondrial protein export machinery. J. Cell Biol. *172*, 553–564.

Gambill, B.D., Voos, W., Kang, P.J., Miao, B., Langer, T., Craig, E.A., and Pfanner, N. (1993). A dual role for mitochondrial heat shock protein 70 in membrane translocation of preproteins. J. Cell Biol. *123*, 109–117.

Gietz, R.D., and Woods R.A. (2002). Transformation of yeast by lithium acetate/single-stranded carrier DNA/polyethylene glycol method. Methods Enzymol. *350*, 87–96.

Haan, C., and Behrmann, I. (2007). A cost effective non-commercial ECL-solution for Western blot detections yielding strong signals and low background. J. Immunol. Methods *318*, 11–19.

Hofmann, K., and Stoffel, W. (1993). TMBASE – A database of membrane spanning protein segments. Biol. Chem. Hoppe-Seyler *374*, 166.

Hünten, S., Kaller, M., Drepper, F., Oeljeklaus, S., Bonfert, T., Erhard, F., Dueck, A., Eichner, N., Friedel, C.C., Meister, G., et al. (2015). p53-regulated networks of protein, mRNA, miRNA, and lncRNA expression revealed by integrated pulsed stable isotope labeling with amino acids in cell culture (pSILAC) and next generation sequencing (NGS) analyses. Mol. Cell. Proteomics *14*, 2609–2629.

Laemmli, U.K. (1970). Cleavage of structural proteins during the assembly of the head of bacteriophage T4. Nature *227*, 680–685.

Longtine, M.S., McKenzie, A. 3rd, Demarini, D.J., Shah, N.G., Wach, A., Brachat, A., Philippsen, P., and Pringle, J.R. (1998). Additional modules for versatile and economical PCR-based gene deletion and modification in *Saccharomyces cerevisiae*. Yeast *14*, 953–961.

Lytovchenko, O., Naumenko, N., Oeljeklaus, S., Schmidt, B., von der Malsburg, K.,

Deckers, M., Warscheid, B., van der Laan, M., and Rehling, P. (2014). The INA complex facilitates assembly of the peripheral stalk of the mitochondrial F_1F_o-ATP synthase. EMBO J. *33*, 1624–1638.

Nielsen, H., Engelbrecht, J., Brunak, S., and von Heijne, G. (1997). Identification of prokaryotic and eukaryotic signal peptides and prediction of their cleavage sites. Protein Eng. *10*, 1–6.

Schägger H. (2006). Tricine-SDS-PAGE. Nat. Protoc. *1*, 16–22.

Schägger, H., and von Jagow, G. (1991). Blue native electrophoresis for isolation of membrane protein complexes in enzymatically active form. Anal. Biochem. *199*, 223–231.

Schägger, H., Cramer, W.A., and von Jagow, G. (1994). Analysis of molecular masses and oligomeric states of protein complexes by blue native electrophoresis and isolation of membrane protein complexes by two-dimensional native electrophoresis. Anal. Biochem. *217*, 220–230.

Sikorski, R.S., and Hieter, P. (1989). A system of shuttle vectors and yeast host strains designed for efficient manipulation of DNA in *Saccharomyces cerevisiae*. Genetics *122*, 19–27.

Thomas, B.J., and Rothstein, R. (1989). Elevated recombination rates in transcriptionally active DNA. Cell *56*, 619–630.

Vögtle, F.N., Wortelkamp, S., Zahedi, R.P., Becker, D., Leidhold, C., Gevaert, K., Kellermann, J., Voos, W., Sickmann, A., Pfanner N., et al. (2009). Global analysis of the mitochondrial N-proteome identifies a processing peptidase critical for protein stability. Cell *139*, 428–439.

Vukotic, M., Oeljeklaus, S., Wiese, S., Vögtle, F.N., Meisinger, C., Meyer, H.E., Zieseniss, A., Katschinski, D.M., Jans, D.C., Jakobs, S., et al. (2012). Rcf1 mediates cytochrome oxidase assembly and respirasome formation, revealing heterogeneity of the enzyme complex. Cell Metab. *15*, 336–347.

Wach, A. (1996). PCR-synthesis of marker cassettes with long flanking homology regions for gene disruptions in *S. cerevisiae*. Yeast *15*, 259–265.

Wiedemann, N., Pfanner, N., and Ryan, M.T. (2001). The three modules of ADP/ATP carrier cooperate in receptor recruitment and translocation into mitochondria. EMBO J. *20*, 951–960.

Table S1. Proteins Identified in Mitochondrial Fractions by Quantitative MS-Based Analysis of Wild-Type Versus *oxa1 cox18* Double Deletion Yeast (see Excel File), Related to Figure 1

Table S2. Yeast Strains Used in This Study, Related to Figures 1, 2 and 3

Strain	Description	Genotype	Source	Number
Wild-type (WT)	YPH499	*MAT*a *ura3-52 lys2-801 ade2-101 trp1-Δ63 his3-Δ200 leu2-Δ1*	Sikorski and Hieter, 1989	1501
Wild-type (WT)	W303-1A *MAT*a; WT for *oxa1-ts* strain	*MAT*a *leu2-3,112 trp1-1 can1-100 ura3-1 ade2-1 his3-11,15*	Thomas and Rothstein, 1989	1045
Wild-type (WT)	YPH499; *pam16::ADE2* pFL39-PAM16; WT for *pam16-3*	YPH499 *pam16::ADE2* pFL39-PAM16	Frazier et al., 2004	3156
Wild-type (WT)	PK82; WT for *ssc1-3* (PK83)	*MATα his4-713 lys2 ura3-52 leu2-3,112 Δtrp1*	Gambill et al., 1993	2501
Wild-type rho^0	YPH499 rho^0; devoid of mitochondrial DNA; generated by ethidium bromide treatment	*MAT*a *ura3-52 lys2-801 ade2-101 trp1-Δ63 his3-Δ200 leu2-Δ1; rho^0*	Pfanner/ Wiedemann Labs	1519
*oxa1*Δ	Deletion of *OXA1* in YPH499 cells	YPH499 *oxa1*::*HIS3MX6*	This study (A.E. Frazier and P. Rehling)	1474
*cox18*Δ	Deletion of *COX18* in YPH499 cells (deletion of ORF (1-951) and 20 base pairs downstream of ORF)	YPH499 *cox18*::*HIS3MX6*	This study (A.E. Frazier and P. Rehling)	1526
*oxa1*Δ *cox18*Δ	Deletion of *OXA1* and *COX18* in YPH499 cells	YPH499 *oxa1::HIS3MX6 cox18::URA3*	This study	3754
oxa1-ts	*oxa1^{ts}* (L240S)	W303-1A *MAT*a *oxa1::OXA1^{L240S}*	Hell et al., 2001; Preuss et al., 2001	2277
Oxa1$_{ProtA}$	Oxa1$_{ProtA}$ (chromosomal)	YPH499 *oxa1*:: *OXA1ProtAHIS3MX6*	Frazier et al., 2006	1522
ssc1-3	PK83	*MATα ade2-101 lys2 ura3-52 leu2-3,112 Δtrp1 ssc1-3(LEU2)*	Gambill et al., 1993	2503
pam16-3	Chromosomal deletion of *PAM16* complemented with temperature-sensitive *pam16-3* allele on plasmid	YPH499 *pam16::ADE2 pFL39-PAM16ts-3*	Frazier et al., 2004	3158